Biophysical Journal
Article

Biophysical Society

# Thick-Filament Extensibility in Intact Skeletal Muscle

Weikang Ma,[1] Henry Gong,[1] Balázs Kiss,[2] Eun-Jeong Lee,[2] Henk Granzier,[2] and Thomas Irving[1,*]
[1]Department of Biological Sciences, Illinois Institute of Technology, Chicago, Illinois and [2]Department of Cellular and Molecular Medicine, University of Arizona, Tucson, Arizona

ABSTRACT Myofilament extensibility is a key structural parameter for interpreting myosin cross-bridge kinetics in striated muscle. Previous studies reported much higher thick-filament extensibility at low tension than the better-known and commonly used values at high tension, but in interpreting mechanical studies of muscle, a single value for thick-filament extensibility has usually been assumed. Here, we established the complete thick-filament force-extension curve from actively contracting, intact vertebrate skeletal muscle. To access a wide range of tetanic forces, the myosin inhibitor blebbistatin was used to induce low tetanic forces in addition to the higher tensions obtained from tetanic contractions of the untreated muscle. We show that the force/extensibility curve of the thick filament is nonlinear, so assuming a single value for thick-filament extensibility at all force levels is not justified. We also show that independent of whether tension is generated passively by sarcomere stretch or actively by cross-bridges, the thick-filament extensibility is nonlinear. Myosin head periodicity, however, only changes when active tension is generated under calcium-activated conditions. The nonlinear thick-filament force-extension curve in skeletal muscle, therefore, reflects a purely passive response to either titin-based force or actomyosin-based force, and it does not include a thick-filament activation mechanism. In contrast, the transition of myosin head periodicity to an active configuration appears to only occur in response to increased active force when calcium is present.

## INTRODUCTION

The sliding filament model of muscle contraction, in which thin and thick filaments slide past each other without changing their length, had as important early evidence the observation that the periodicities of the thick and thin filaments did not change when muscle contracts (1–4). This led researchers to consider the myofilaments as being inextensible, with essentially all of the axial elasticity in the myofilaments residing in the cross-bridges. This was a highly influential idea that later turned out to be incorrect. Huxley (5) and Wakabayashi (6) showed that by accurately measuring the higher-order actin and myosin-based meridional reflections, changes in the length of both thin and thick filaments of ~0.3% at full isometric tension could be observed in response to activation of the muscle. This new insight required a major reassessment of the then-popular models of muscle contraction and in particular the interpretation of force transients that occur upon step-length changes (7,8).

Thick-filament extensibility has been generally assumed to be a fixed value, i.e., the relationship between force and extension is linear. The extensibility in actively contracting intact muscle at high tetanic tension has been estimated to be 11–16 m/N (9). More recently, however, in passively stretched skinned rabbit psoas muscle, it was shown that thick filaments under low tension are much more extensible, around 85 m/N, at the low tensions generated by passive stretch as compared to the greatly reduced extensibilities observed at high tensions during isometric tetanic contraction (10). These authors proposed that the discrepancy between these two numbers could be reconciled if there was a nonlinear relationship between thick-filament extension and tension. In their study, however, this relationship could not be conclusively demonstrated because of the limited range of tensions used (10). The observation that thick filaments appear to be more extensible at low tension than at high tension is, however, consistent with results obtained from synthetic rabbit thick filaments containing only myosin. Synthetic thick filaments are ~10 times more compliant at low tension than at high tension (11), but because of the lack of other thick-filament-associated proteins, studies of synthetic thick filament might not reflect native filament extensibility.

Titin is a giant sarcomeric protein (~2.9–3.8 MDa) (12,13) that spans half of the sarcomere from the Z disk

*Submitted May 7, 2018, and accepted for publication August 29, 2018.*
*Correspondence: irving@iit.edu
Editor: David Warshaw.
https://doi.org/10.1016/j.bpj.2018.08.038

all the way to the M-band (14). Titin is a long and elastic protein that acts as a molecular spring that maintains the structural integrity of the sarcomere (15–18). Titin closely interacts with the thick filament inside the A-band and plays an important role in passive force generation (19). It is also involved in mechanosensing within signaling pathways (20,21). Titin-based passive tension had been shown to strain the thick-filament backbones and to alter the helical arrangements of the myosin heads in cardiac muscle, shedding light on the Frank-Starling law mechanisms at the molecular level (22). The details of the interactions between titin and thick-filament proteins in intact thick filaments in skeletal muscle remain to be established.

The primary goal of the current study was to determine the complete thick-filament force-extension curve from actively contracting and passive intact vertebrate skeletal muscle. To access a wide range of tetanic forces, blebbistatin, a myosin inhibitor (23), was used to induce low tetanic forces along with the higher tensions obtained from tetanic contractions of untreated muscle, delivering a range of tensions. We found that the extensibility of the thick filament is indeed nonlinear, so assuming a single value for thick-filament extensibility is not justified. Our data indicate that nonlinear thick-filament extensibility is independent of whether the tension is generated passively by stretch or actively by cross-bridges. Although increasing active tension is associated with a transition in the spacing of myosin heads toward an "active" configuration, no such change is seen in passively stretched muscle.

## MATERIALS AND METHODS

### Experimental apparatus

A combined servo motor/force transducer (Model 6350; Cambridge Technology, Bedford, MA) was mounted on an *X-Y-Z* positioner adjacent to the chamber holder. The combined motor/force transducer head was connected to a dual-mode controller (300C; Aurora Scientific, Aurora, Canada). Intact muscles were placed in the experimental chamber filled with oxygenated Ringer solution and were subsequently activated with a high-power biphasic current stimulator (model 701A; Aurora Scientific). The whole system (Fig. 1) was controlled by an ASI 610A data acquisition and control system (Aurora Scientific).

### Muscle preparations

The mice used to determine thick-filament extensibility in actively contracting muscle were C57BL/6 mice (male, 10–15 weeks). All animal experiments were governed by protocols approved by the University of Arizona and Illinois Institute of Technology Institutional Animal Care and Use Committees. Mice were euthanized by carbon dioxide inhalation and cervical dislocation. The skin was removed to expose the muscles and separate the hind limbs. During dissection, the muscles were kept on ice and moist with the application of Ringer solution (Ringer's solution contained 145 mM NaCl, 2.5 mM KCl, 1.0 mM $MgSO_4$, 1.0 mM $CaCl_2$, 10.0 mM HEPES, 11 mM glucose (pH 7.4)) at regular intervals. The hind limbs were placed in a dish filled with Ringer's solution perfused with 100% oxygen. For electrically stimulated wild-type mouse muscle, the hind limbs were pinned to the dish with insect pins and both the soleus and extensor digitorum longus (EDL) were dissected out carefully in Ringer's solution, leaving as much tendon as possible attached on both ends. Passive stretch experiments followed the same procedure, but in this case, only the EDL muscle was used. Silk sutures were used to tie to the tendons on both ends of the muscle. The sutures were tied to the force transducer and a fixed hook inside the chamber (see Fig. 1). The muscle was adjusted to the desired length by the *X-Y-Z* positioner attached to the force transducer before the x-ray and mechanical experiment. The experimental chamber was maintained at room temperature (22°C) and continuously oxygenated during the experiment.

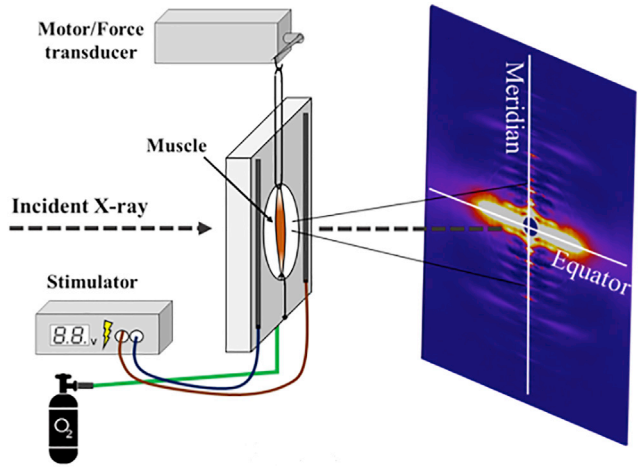


FIGURE 1 Experimental setup. The isolated intact muscle is mounted in a fluid-filled chamber, sutured at one end to a fixed hook and at the other end to a hook connected to a combined servo motor/force transducer system. The sample was then aligned with the x-ray beam. Force, length, and x-ray patterns were synchronously recorded while the muscle was either passively stretched or tetanized. To see this figure in color, go online.

### X-ray diffraction

X-ray diffraction experiments were done using the small angle x-ray diffraction instrument on the BioCAT beamline 18ID at the Advanced Photon Source, Argonne National Laboratory, Lemont, IL (24). The x-ray beam energy was set to 12 keV (0.1033 nm wavelength) at an incident flux of $\sim 10^{13}$ photons per second in the full beam. The x-ray beam was focused to $\sim 250 \times 250$ $\mu$m at the sample position and to $\sim 130 \times 60$ $\mu$m at the detector. The specimen to detector distance was $\sim 1.8$ m. A high-sensitivity, high-readout-speed (up to 500 Hz) Pilatus 3 1 M detector (Dectris, Baden-Daettwil, Switzerland) with an active area of 168.7 mm $\times$ 179.4 mm with 172 $\times$ 172 $\mu$m pixels was used to collect the x-ray patterns.

### Experimental protocols

For experiments in actively contracting muscle, a short tetanic contraction was performed to test the sutures (0.5 s tetanus contraction at a 100 Hz pulse frequency, 2 ms pulse width, followed by a 0.2 s initial delay). The muscle was then stretched to $L_0$, defined as the optimal muscle length at which the maximal twitch force was generated. For the mechanical and x-ray experiments, the muscles were activated by a 100 Hz pulse frequency, 2 ms pulse width stimulation for a 3 s isometric tetanic contraction followed by at least a 10 min resting period. The x-ray shutter was kept open during the entire protocol, including 1 s of low force data before and after the tetanus, with the detector continuously collecting data frames with a 1 ms exposure time and 2 ms frame period. The muscle was oscillated in the beam during the exposure to spread the x-ray dose and reduce radiation damage.

For experiments on passive muscle, the EDL muscle was initially at optimal length, the same as in the actively contracting experiment. 100 x-ray images were taken, each with a 10 ms exposure time and a 100 ms readout time. Force was recorded continuously. The muscle was then stretched by 15% from optimal length with the motor at a constant speed (10%/min) and the force allowed to stabilize. Another 100 images were taken at the same frame rate and exposure time. This procedure was then repeated with a larger amplitude stretch (25%, 35%, and on occasion higher, but never exceeding a maximal stretch of 60% over optimal length).

### Blebbistatin treatment

Blebbistatin was used to access low active-tension levels by partially inhibiting actomyosin interaction in intact muscle. 100 $\mu$L of 7.5 mM blebbistatin (Cayman Chemical, Ann Arbor, MI) dissolved in dimethyl sulfoxide was added to the chamber containing ~10 mL Ringer's solution and incubated for 15–30 min. Because blebbistatin is sensitive to short wavelength light but stable at 500 nm (25), experiments were performed in the dark, except for a low-power red light-emitting diode light that was used during muscle alignment.

### Postexperiment muscle treatment

After each mechanical and x-ray experiment, the muscle was recovered for cross-sectional area calculation. The cross-sectional area was calculated according to the muscle length and the muscle mass, assuming a muscle density of 1.06 g/mL (26,27). The muscle was placed back in relaxation solution and was then stretched to the experimental length and fixed in 10% formalin for 10 min. The sarcomere length was recorded by using a video sarcomere length system (model 900B; Aurora Scientific) from fixed fiber bundles throughout the entire muscle cross section.

### Titin-based tension estimation

Titin-based tension was estimated by measuring the difference between total passive tension and postskinned, thick and thin filaments extracted, and passive tension from the same kind of muscle. Mouse EDL muscles were divided into four smaller muscle bundles by separating the tendons at one end of the muscle. The fiber bundle was attached to T-clips on both ends, and it was then stretched to 15, 25, and 35% over optimal length as was done in the passively stretched intact muscle experiments. They were demembranated in a relaxing solution that contained 1% Triton X-100 for 3 h with three buffer changes. The fiber bundles were then treated with high-concentration KCl and KI solutions to depolymerize thick and thin filaments; for details, see our previous work (18). The mechanical experiments were then repeated to determine the passive tension due to extracellular components. Titin-based passive tension was determined as the difference between total passive tension and extracellular-based passive tension (21).

### Data analysis

The x-ray detector data were saved as 32-bit tagged image file format images and analyzed using data analysis programs belonging to the MuscleX software package developed at BioCAT (28). For thick-filament extensibility measurements under steady-state conditions, first the individual images from resting patterns (0–1 s) were averaged together into one image. Then, the individual images taken during the plateau of isometric tetanus (from the time maximal force is reached to the end of stimulation) were averaged into one image. It was these averaged images that were used in subsequent analysis. For analysis of time-resolved data, each frame was analyzed individually. The spacings and intensities of meridional reflections on either side of the pattern were obtained using the "Diffraction Centroids" program. "Diffraction Centroids" estimates the peak position as the centroid of the intensity of the top half of the diffraction peak. This measure, as used in Huxley et al. (5), has the advantage of being model independent and insensitive to noise and the detailed shape of the peak.

## RESULTS

### Thick-filament extensibility in actively contracting mouse skeletal muscle

There is general consensus that the intensity of the third order myosin meridional (M3; ~14.3 nm) reflection is dominated by contributions from the myosin heads and that the M6 and higher-order myosin reflection are dominated by contributions from structures within the backbone (9,29,30). Although it is possible that configurations of myosin heads and/or actomyosin interactions are influencing the higher-order myosin meridionals, these are likely to be secondary and relatively minor effects. For this reason, changes in the spacing of the M6 (7.2 nm) and higher-order meridional reflections have been used to study the extensibility of thick filaments as a function of active force in frog muscle (6,29,30) and as a function of titin-based passive tension in skinned rabbit muscle (10). In intact mouse muscle, both the M6 (at 7.15 nm) and the M15 (at 2.86 nm) can be well resolved in both the passive and active states (Fig. 2, the *right half* shows the contracting pattern and the *left half* shows the resting pattern taken before the contraction). The 15th myosin meridional reflection is particularly useful, as it is far from the beam center and allows accurate estimates of small differences in the thick-filament periodicity. Fig. 3 shows a plot of the percent change of the M6 spacing (7.15 nm) as a function of tetanic tension superimposed with that of the M15 (2.86 nm) meridional reflection. Results indicate that thick-filament extensibility can be estimated from both reflections, although the 2.86 nm meridional reflection measurements, being farther from the center, may be measured more accurately and consequently the data show less scatter.

The percentage change of the M15 reflection (2.86 nm) is shown as a function of tetanic tension in Fig. 4 *A* for soleus and Fig. 4 *B* for EDL muscle, respectively. Both muscle types show a clear nonlinear relationship between thick-filament backbone periodicity and tension generated by a tetanic contraction. The slope of the force-extension plot at low stress (<50 mN/mm$^2$) in both EDL and soleus corresponds to an extensibility of ~80 m/N consistent with our previous findings (10). In contrast, the extensibility of skeletal muscle at high stress, estimated from the slopes of the lines at tensions >80 mN/mm$^2$, are 15.6 $\pm$ 3 and 13.5 $\pm$ 3.7 m/N for EDL and soleus muscle, respectively, comparable to the literature values (11–16 m/N (9,10)). Soleus and EDL muscles have a similar shape but are not identical, especially at high tensions. The architectural properties and myofibrillar densities are likely different in soleus and EDL muscles (26), so direct quantitative

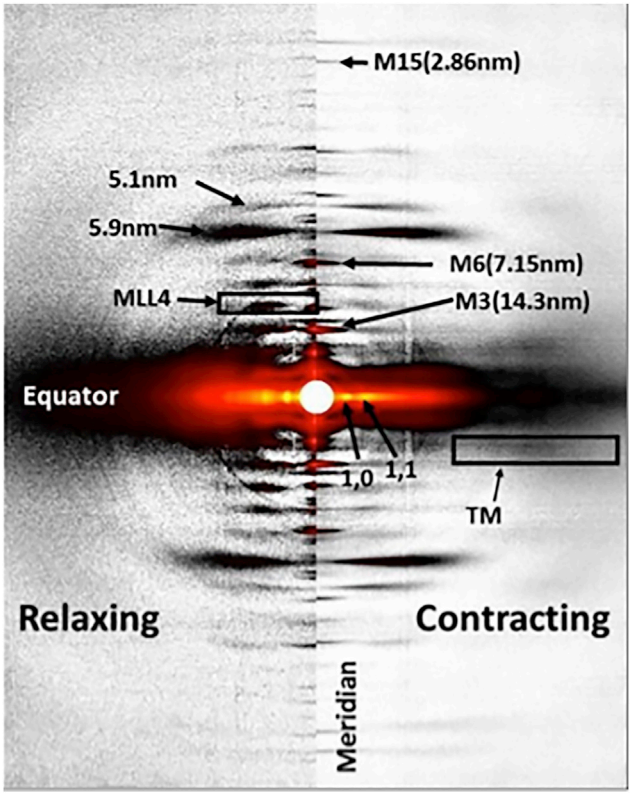


FIGURE 2 X-ray diffraction pattern from resting (*left*) and activated (*right*) mouse soleus muscle. The 1,0 and 1,1 equatorial reflections are indicated. The M3 reflection on the meridian arises from the 14.3 nm myosin axial displacement. The M6 reflection at 7.15 nm arises primarily from structures within the thick-filament backbone. The meridional reflection at 2.86 nm is the 15th order of the myosin repeat. The M4 layer line is derived from the helical arrangement of myosin heads around the thick-filament backbone. The reflection on the second actin layer line, arising from tropomyosin, is indicated as TM. See text for additional details.

comparison of thick-filament extensibility between soleus and EDL muscles would require more detailed knowledge of the proportion of myofibrillar area per muscle cross-sectional area (see also Discussion). However, both muscle types show a clear nonlinear relationship between thick-filament backbone periodicity and active tension.

## Thick-filament extensibility in passively stretched skeletal muscle

To study how passive tension affects thick-filament strain, the 2.86 nm myosin-reflection spacing changes were plotted against the total passive tension generated by stretching EDL muscle in its passive state (Fig. 5 *A*, *filled circles*). The overall shape of the obtained curve resembles that of the active tension curve (Fig. 5 *A*, *open circles*) but has a rightward shift compared to the active tension curve. Because not all of the total passive tension is titin-based, we determined the proportion of passive tension attributable to titin and extracellular matrix (see Materials and

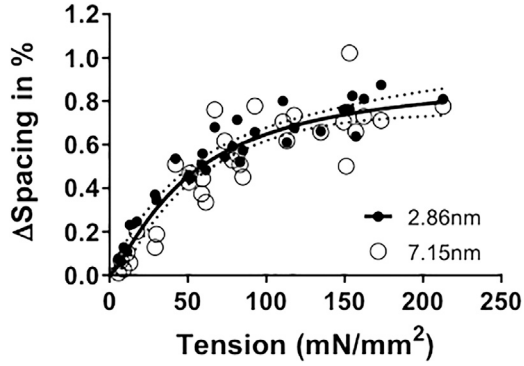


FIGURE 3 Thick-filament backbone reflections in soleus muscle as a function of active tension. Relative changes in the spacing of the 2.86 nm (M15) and 7.15 nm (M6) x-ray reflections as a function of active tension are indistinguishable, but the 2.86 nm reflections appear less scattered than the 7.15 nm reflections. The fit to a Hill model is shown (*heavy line*) along with 95% confidence levels (*dotted lines*).

Methods). We found that within the length range that was studied, titin accounted for 63% of the total passive tension. When the 2.86 nm myosin reflection spacing changes are plotted as a function of titin-based tension, the relationship is now indistinguishable from that of actively contracting muscle (Fig. 5 *B*). Thus, the tension-extension curve of the thick filament is nonlinear, irrespective of whether the tension is titin-based passive tension or cross-bridge-based active tension.

## M3 meridional reflection

To explore whether passive tension also impacts the disposition of the myosin heads, we studied the M3 meridional x-ray reflection. This reflection is attributed to the ~14.3 nm axial displacement of successive myosin heads along their helical tracks on the thick filament (3,31), with the intensity coming primarily from the mass of the myosin heads, whereas the M6 reflection intensity arises primarily from structures within the thick-filament backbone (9,30). The M3 spacing in contracting mouse muscle increased little with active tension when tensions were small (<~30 mN/mm$^2$), but at high

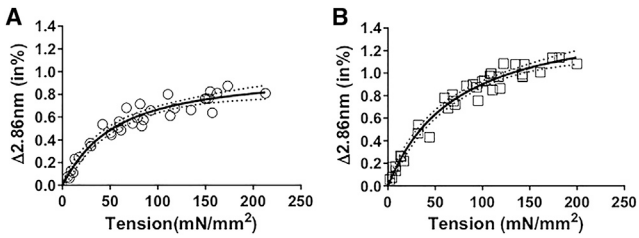


FIGURE 4 Thick-filament extensibility in tetanized soleus (*A*) and EDL (*B*) skeletal muscle. The 2.86 nm spacing change as a function of tetanic tension is plotted. Both EDL and soleus muscle showed a nonlinear relationship between the 2.86 nm spacing change and active tension. The fits to a Hill model are shown (*heavy line*) along with 95% confidence levels (*dotted lines*).

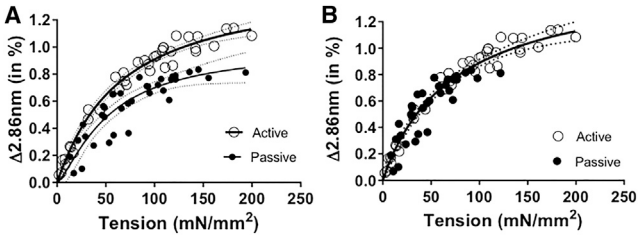


FIGURE 5 Thick-filament extensibility in passively stretched muscle compared to that in active muscle. (*A*) The spacing of the 2.86 nm reflection as a function of total passive tension (*filled circles*) and active tension (*open circles*) in passively stretched and actively contracting EDL muscle, respectively. The thick-filament-extensibility curve from actively contracting muscle has a similar shape to that of passive stretched muscle, but curves do not overlap. (*B*) The 2.86 nm myosin-reflection changes as a function of titin-based passive tension in passively stretched muscle were indistinguishable from the spacing changes in actively contracting EDL muscle as a function of active tension. The fits to a Hill model are shown (*heavy line*) along with 95% confidence levels (*dotted lines*).

tension, the increase was rapid, and a maximal spacing change of ~1% was reached at a tension of ~100 mN/mm$^2$ (Fig. 6 *A*). The M3 spacing as a function of active tension data was fitted to both a linear function and a Hill model, with the Hill model providing a significantly better fit ($p < 0.05$ for nonlinear curve fit) with a half-maximal spacing change at ~60 mN/mm$^2$. In passively stretched muscle—in which, as described above, the M15 spacing shows a systematic increase with increasing passive tension—the M3 spacing shows no such systematic increase (Fig. 6 *B*). Thus, passive tension increases the average periodicity of structures within the thick-filament backbone but does it in such a way that the average axial displacement of the myosin heads does not change.

### Spacing changes in M3 and M6 reflections in time-resolved experiments

X-ray patterns were collected with a 1 ms exposure time and 1 ms readout (500 Hz frame rate) during the tension rise after tetanic stimulation. The M3 and M6 spacings and tension were plotted as a function of time. The M6 starts to increase at the same time as active force development (Fig. 7, *squares and diamonds*), but the M3 spacing (*circles*) starts to increase ~6 ms later. The M3 spacing as a function of time can be fitted with a Hill model with a half-maximal spacing change at 0.019 s, corresponding to an active tension of ~60 mN/mm$^2$.

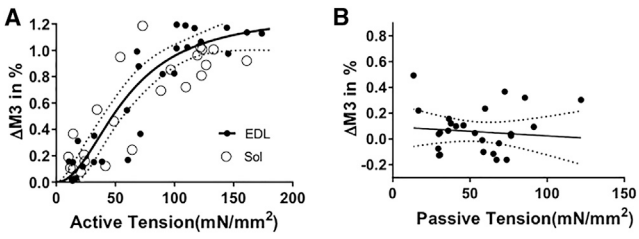


FIGURE 6 M3 meridional reflection spacing changes as a function of active (*A*) and titin-based passive tension (*B*). In active muscle, the M3 spacing changes from both EDL (*solid circles*) and soleus muscle (*open circles*) as a function of tetanic tensions. The fit to a Hill model is shown (*heavy line*) along with 95% confidence levels (*dotted lines*) (*b*). M3 spacing as a function of passive tension in EDL muscle. The M3 spacing did not increase with an increase in passive tension.

## DISCUSSION

### Nonlinear thick-filament extensibility in actively contracting muscle

Knowledge of thick-filament extensibility is critical for determining cross-bridge cycling kinetics and examining mechanisms of muscle contraction (32–34). Small and rapid length oscillations applied to activated muscle have been widely used to estimate muscle stiffness and cross-bridge numbers and extensibility (35–38). However, the early studies were based on the assumption that the thick filament is inextensible, as it appeared from initial x-ray studies (1–4). The subsequent finding that myofilaments have significant elasticity (5,6) is now widely used in the interpretation of cross-bridge kinetics studies (39,40). In all of these cases, however, the myofilament elasticity is assumed to have a single fixed value. Fusi and colleagues concluded that, in frog muscle, myofilament extensibility accounts for two thirds of total fiber extensibility and cross-bridges for the remaining one third (41), but another study showed the opposite results (40). The thick-filament extensibility in passively stretched skinned skeletal muscle fibers (10) was observed to be much higher than found in tetanically contracted intact skeletal muscle (9). Because tetanic contraction in intact skeletal muscle generates more tension than passively stretched skinned skeletal muscle fibers, the authors proposed that the thick filament is more extensible at low tension than at high tension (10). These studies,

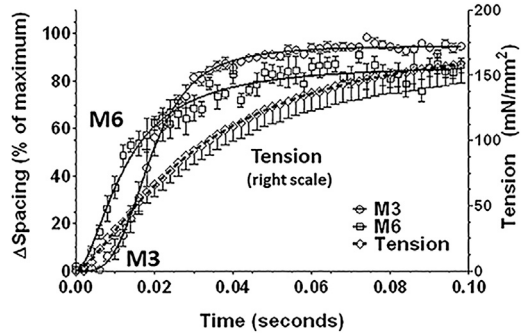


FIGURE 7 Time courses of the M3 and M6 meridional reflection spacing changes (*left scale*) and tetanic tension (*right scale*). Relative spacing changes as a percentage of the maximal changes are shown for the M3 (*circles*) and M6 (*squares*) meridional x-ray reflections as compared to active tension (*diamonds*) as a function of time after stimulation in intact mouse EDL muscle. The solid and dotted lines are fits to a Hill model.

however, did not address whether or not the extensibility of the thick filament is different in actively contracting versus passive stretched muscle. Direct measurements of thick-filament extensibility over a wide range of tensions, in both active and passive muscle, were needed to resolve these questions and discrepancies.

Here, we demonstrate that thick-filament extensibility in contracting intact skeletal muscle is indeed nonlinear when examined over the range of tensions from zero to maximal isometric tension. Similar relative thick-filament extensions with force (~80 m/N) were observed using the M6 spacing changes as previously used by Irving et al. (10) to those measured from the 2.86 nm meridional reflections. The extensibility of skeletal muscle at high tension levels (>80 mN/mm$^2$) was found to be 13–16 m/N, within the range of literature values (11–16 m/N (9,10)), again assuming a linear relationship. Rather than two linear functions, however, the thick-filament-extensibility curve seems more likely to be a continuous, nonlinear function (in Figs. 3, 4, and 5, Hill functions were assumed) of increasing force. It should be noted that a similar nonlinear force-extension curve in active frog muscle was reported but not discussed as such by Linari and colleagues in Fig. 3 *d* of (42). Similarly, Brunello and colleagues (38) reported a linear force-extension relation, again in active frog muscle, above 0.4 T0 (maximum isometric tension) that diverges from linearity at lower forces.

There appeared to be a significant difference in thick-filament extensibility as a function of tetanic tension in soleus muscle and EDL muscle (Fig. 4). Soleus muscle contains ~40% slow fibers, whereas EDL contains ~90% fast fibers, and it may be that the myofilament density in EDL and soleus muscles is different (43–45). It is likely to be more informative to plot thick-filament extensibility against force per thick filament to determine whether or not extensibility of the thick filaments is the same or different in the EDL and soleus muscles. This will require detailed knowledge of the proportion of myofibrillar area per cross-sectional area in each muscle, and this will be addressed in future studies.

Why is the force-extension curve nonlinear? It is not clear whether the interactions responsible for the nonlinear extensibility are intramolecular, intermolecular, or both. The changes in axial spacing from rest to full isometric tension, at the level of the 14.3 nm axial-head separation (in resting muscle), are ~0.1–0.2 nm. At the individual bond level, the changes will be subtle indeed, well within normal variations in bond lengths. Although one might expect, a priori, that intramolecular extension as a function of force over short distances will be approximately linear, intermolecular interactions could well be more complex. Recent results from the Taylor group (46) show that the myosin molecules, at least in insect flight muscle but probably in all muscles, do not wind around each other but form parallel arrangements that they call ribbons held together by noncovalent interactions along their length. It may be that the relatively high extensibilities at low thick-filament strains are due to rearrangement of the weakly bound rods in the ribbons under strain. Because extension continues as strain increases, the molecules may become more entangled and the whole structure becomes relatively inextensible. At that point, additional force would presumably go toward stretching individual bonds in the myosin rods. This could explain the much stiffer filaments and the approximately linear relation of thick-filament extension at high forces. This hypothetical scenario would need verification in future experiments.

## Thick-filament extensibility and passive tension

Titin inside the A-band closely interacts with the thick filament (20), and titin is believed to strain thick filaments when the muscle is stretched (10,22). Titin when stretched to different lengths will consequently strain the thick filaments to different extents. The estimates for thick-filament extensibility obtained in this study from actively contracting muscle at low tension levels were close to that from the previous study in skinned passively stretched rabbit psoas muscle (10). When total passive force was converted to titin-based force, the thick-filament extensibility from passively stretched EDL muscle was not statistically different from actively contracting muscle, and they are both similarly nonlinear (Fig. 5 *B*). Thus, the nonlinearity of the thick-filament force-extension curve in skeletal muscle appears to reflect a purely passive response to either titin-based force or active force.

It should be noted that the active muscle experiments are all done at the same sarcomere length, whereas different amounts of titin-based passive tension are generated by stretching the muscles to different sarcomere lengths. A concern might be that there may be structural changes with increasing sarcomere length other than increased titin-based passive tension that could confound the comparison with active muscle. Identically shaped relationships in active muscle and passively stretched muscle suggests that the nonlinear extensibility of the backbone is a fundamental property of the thick filament.

As discussed above, when comparing the soleus and EDL muscles, the number of thick filaments per unit cross-sectional area will differ because of differences in internal architecture, precluding studying the extensibility as a function of thick-filament cross-sectional area. Additionally, the strain at a particular point on the thick filament most likely will vary. In active muscle, insofar as the cross-bridges are truly independent force generators, there will be a gradient in strain from the tip of the filament, where the strain is zero, to the edge of the H-zone, where the force will be maximal. The steepness of the gradient will depend on the degree of filament overlap. Under our conditions, the average strain in the thick filament would be ~0.6 times

the measured force per unit area delivered by the muscle, all other things being equal. In passive muscle, one may start by assuming that the passive force generated by titin is exerted at the ends of the filaments and propagated to provide a uniform strain throughout the filament. However, given that titin makes multiple contacts along the thick filament (47), there could be local strain gradients in passive muscle as well. Titin also makes contacts with the thin filaments in the I-band (48), which might allow some of the strain to be borne by the thin filaments. In either active or passive muscle, other connections between the thick and thin filaments may alter strain distributions. Myosin-binding protein C is proposed to have interactions with actin under resting conditions that would be present in the C-zone of the thick filament and absent in the D-zone (49). Similarly, cross-bridges in active muscle could also redistribute longitudinal strain radially to the thin filaments. All these interactions could serve to redistribute strain in hard-to-predict ways. Although the coincidence of the passive and active force extension curve shown in Fig. 5 *B* is remarkable, it cannot presently be concluded that the thick-filament strain curves are also identical without more information from future studies. In summary, although local thick-filament strain gradients that are different in passive and active muscle are likely to exist, from this work, it can be concluded that the thick-filament force-extension curves in active and passive muscle are similarly nonlinear.

### Thick-filament-based activation mechanisms

The widely accepted steric blocking model of thin-filament regulation states that calcium first binds to troponin, which then allows tropomyosin to move on the thin filament, uncovering myosin-binding sites on actin to allow contraction to occur (50,51). Recently, there has been increased interest in thick-filament-based activation mechanisms, as has been recently reviewed (52). It has been known for a long time (53) that there is a change in the myosin meridional reflections associated with going from the resting to the isometrically contracting state, suggesting that the "active" thick filament is in a different structural state than in resting muscle. More recently, Linari et al. (42) proposed that strain in the myosin thick-filament backbone acts as a mechanosensor to "turn on" the thick filament, with the M3 spacing change being one of the hallmarks of the muscle "on" state (42). In this model, a small number of cross-bridges are always available to interact with actin, and upon activating the thin filament, they interact with actin first, generating force and increasing strain in the thick filament. When this strain reaches some transition value to the long-periodicity "on" structure, this is proposed to release the larger population of motors required for high-load contraction (42).

In these experiments with contracting muscle, a nonlinear change in M3 spacing with increasing tension is indeed observed (Figs. 6 *A* and 7), indicating a stepwise change in spacing (at ~60 mN/mm$^2$) when going from the low-force region to a high-force region with force either altered by blebbistatin treatment or during the tension rise of a normal tetanic contraction. The average axial displacements, as reflected in the M3 myosin meridional reflection, of myosin heads in passive muscle are, however, unaffected by thick-filament strain (Fig. 6 *B*).

The force-extension curve of the thick-filament backbone, as reflected in the spacing changes in either the M6 or the M15 myosin meridional reflections, are similarly nonlinear in active and passive muscle (Fig. 5 *B*). Thus, the nonlinearity of the thick-filament force-extension curve in skeletal muscle appears to reflect a purely passive response to either titin-based force or active force. The lack of stepwise transition in M3 spacing with passive tension indicates that the transition of myosin heads to an active configuration is, therefore, not a necessary consequence of increased thick-filament strain. Reconditi and colleagues (38) also examined M3 spacing changes as a function of sarcomere length in frog muscle. They did not measure titin-based passive tension, but the sarcomere-length changes they chose would have likely involved a similar range of passive tensions as in our study. In their case, there was a systemic increase (~0.3%) in M3 spacing with increasing sarcomere length (and hence passive tension), but they also did not see a stepwise transition to the much larger "on" state spacing.

The results shown here, therefore, demonstrate that the thick-filament "turning on" mechanism, whatever it is, cannot rely only on the degree of thick-filament strain but must involve other mechanisms as well. An appealing hypothesis, as suggested by Reconditi and colleagues (54), is that interactions of myosin-binding protein C with the thin filament communicate the activation state of thin filament early after calcium binding, leading to a structural transition to the "on" state after a delay (38). Another possibility might be that when a significant number of force-producing myosin heads are recruited, this disrupts the resting surface lattice of the myosin heads and their interactions with each other, titin, and the backbone. This then allows for more force producing heads to be recruited from their ordered arrangement around the thick-filament backbone to a configuration able to bind actin in a cooperative process. In any case, rather than being the cause of thick-filament activation as in the Linari et al. model (42), it appears that nonlinear thick-filament strain in contracting muscle is simply an effect of active force development responding in the same way as it would to an applied passive force.

## CONCLUSIONS

The force-extension relationship for skeletal muscle follows a similar, nonlinear relationship with either active tension or

titin-based passive tension; assuming a single value for thick-filament extensibility at all tension levels is therefore not justified. Although the myosin head periodicity (M3) and the level of thick-filament strain (M6/M15) increase with different levels of force in active muscle, which is consistent with a thick-filament-based activation model, passively stretched mouse muscle shows no such transition in myosin head periodicity. The nonlinear thick-filament force-extension curve in skeletal muscle, therefore, appears to reflect a purely passive, albeit nonlinear, response to titin-based strain and not an activation-related structural change.

## AUTHOR CONTRIBUTIONS

W.M., B.K., T.I., and H. Granzier designed the research. W.M., B.K., H. Gong, and E.-J.L. performed the research. W.M. and H. Gong analyzed the data. W.M. and T.I. wrote the manuscript. T.I. and H. Granzier edited the manuscript.

## ACKNOWLEDGMENTS

The authors wish to thank Dr. S. Mijailovich for helpful discussions.

The research was supported by grant R01AR073179 and R01HL115988 to H.G. Use of the BioCAT facility was supported by grant 5 P41 GM103622 from the National Institute of General Medical Sciences of the National Institutes of Health. Use of the Pilatus 3 1 M detector was provided by grant 1S10OD018090-01 from the National Institutes of Health. This research used resources of the Advanced Photon Source, a U.S. Department of Energy Office of Science User Facility operated for the Department of Energy Office of Science by Argonne National Laboratory under Contract No. DE-AC02-06CH11357.

## REFERENCES

1. Huxley, H. E. 1953. X-ray analysis and the problem of muscle. *Proc. R. Soc. Lond. B Biol. Sci.* 141:59–62.
2. Huxley, H. E. 1973. Structural changes in actin- and myosin-containing filaments during contraction. *Cold Spring Harb. Symp. Quant. Biol.* 37:361–376.
3. Huxley, H. E., W. Brown, and K. C. Holmes. 1965. Constancy of axial spacings in frog sartorius muscle during contraction. *Nature.* 206:1358.
4. Elliott, G. F., J. Lowy, and B. M. Millman. 1965. X-ray diffraction from living striated muscle during contraction. *Nature.* 206:1357–1358.
5. Huxley, H. E., A. Stewart, …, T. Irving. 1994. X-ray diffraction measurements of the extensibility of actin and myosin filaments in contracting muscle. *Biophys. J.* 67:2411–2421.
6. Wakabayashi, K., Y. Sugimoto, …, Y. Amemiya. 1994. X-ray diffraction evidence for the extensibility of actin and myosin filaments during muscle contraction. *Biophys. J.* 67:2422–2435.
7. Goldman, Y. E., and A. F. Huxley. 1994. Actin compliance: are you pulling my chain? *Biophys. J.* 67:2131–2133.
8. Huxley, A. F., and S. Tideswell. 1996. Filament compliance and tension transients in muscle. *J. Muscle Res. Cell Motil.* 17:507–511.
9. Reconditi, M. 2006. Recent improvements in small angle X-ray diffraction for the study of muscle physiology. *Rep. Prog. Phys.* 69:2709–2759.
10. Irving, T., Y. Wu, …, H. Granzier. 2011. Thick-filament strain and interfilament spacing in passive muscle: effect of titin-based passive tension. *Biophys. J.* 100:1499–1508.
11. Dunaway, D., M. Fauver, and G. Pollack. 2002. Direct measurement of single synthetic vertebrate thick filament elasticity using nanofabricated cantilevers. *Biophys. J.* 82:3128–3133.
12. Maruyama, K. 1997. Connectin/titin, giant elastic protein of muscle. *FASEB J.* 11:341–345.
13. Wang, K. 1996. Titin/connectin and nebulin: giant protein rulers of muscle structure and function. *Adv. Biophys.* 33:123–134.
14. Fürst, D. O., M. Osborn, …, K. Weber. 1988. The organization of titin filaments in the half-sarcomere revealed by monoclonal antibodies in immunoelectron microscopy: a map of ten nonrepetitive epitopes starting at the Z line extends close to the M line. *J. Cell Biol.* 106:1563–1572.
15. Wang, K., R. Ramirez-Mitchell, and D. Palter. 1984. Titin is an extraordinarily long, flexible, and slender myofibrillar protein. *Proc. Natl. Acad. Sci. USA.* 81:3685–3689.
16. Trinick, J., and L. Tskhovrebova. 1999. Titin: a molecular control freak. *Trends Cell Biol.* 9:377–380.
17. Gregorio, C. C., H. Granzier, …, S. Labeit. 1999. Muscle assembly: a titanic achievement? *Curr. Opin. Cell Biol.* 11:18–25.
18. Granzier, H. L., and T. C. Irving. 1995. Passive tension in cardiac muscle: contribution of collagen, titin, microtubules, and intermediate filaments. *Biophys. J.* 68:1027–1044.
19. Trombitás, K., J. P. Jin, and H. Granzier. 1995. The mechanically active domain of titin in cardiac muscle. *Circ. Res.* 77:856–861.
20. Trinick, J. 1996. Titin as a scaffold and spring. Cytoskeleton. *Curr. Biol.* 6:258–260.
21. Granzier, H. L., and S. Labeit. 2004. The giant protein titin: a major player in myocardial mechanics, signaling, and disease. *Circ. Res.* 94:284–295.
22. Ait-Mou, Y., K. Hsu, …, P. P. de Tombe. 2016. Titin strain contributes to the Frank-Starling law of the heart by structural rearrangements of both thin- and thick-filament proteins. *Proc. Natl. Acad. Sci. USA.* 113:2306–2311.
23. Farman, G. P., K. Tachampa, …, P. P. de Tombe. 2008. Blebbistatin: use as inhibitor of muscle contraction. *Pflugers Arch.* 455:995–1005.
24. Fischetti, R., S. Stepanov, …, G. B. Bunker. 2004. The BioCAT undulator beamline 18ID: a facility for biological non-crystalline diffraction and X-ray absorption spectroscopy at the advanced photon source. *J. Synchrotron Radiat.* 11:399–405.
25. Kolega, J. 2004. Phototoxicity and photoinactivation of blebbistatin in UV and visible light. *Biochem. Biophys. Res. Commun.* 320:1020–1025.
26. Burkholder, T. J., B. Fingado, …, R. L. Lieber. 1994. Relationship between muscle fiber types and sizes and muscle architectural properties in the mouse hindlimb. *J. Morphol.* 221:177–190.
27. Narici, M. V., L. Landoni, and A. E. Minetti. 1992. Assessment of human knee extensor muscles stress from in vivo physiological cross-sectional area and strength measurements. *Eur. J. Appl. Physiol. Occup. Physiol.* 65:438–444.
28. Jiratrakanvong, J., J. Shao, …, G. Agam. 2018. MuscleX: software suite for diffraction X-ray imaging V1.13.1. doi:10.5281/zenodo.1195050.
29. Huxley, H. E. 2004. Recent X-ray diffraction studies of muscle contraction and their implications. *Philos. Trans. R. Soc. Lond. B Biol. Sci.* 359:1879–1882.
30. Linari, M., G. Piazzesi, …, V. Lombardi. 2000. Interference fine structure and sarcomere length dependence of the axial x-ray pattern from active single muscle fibers. *Proc. Natl. Acad. Sci. USA.* 97:7226–7231.
31. Elliott, G. F., J. Lowy, and B. M. Millman. 1967. Low-angle x-ray diffraction studies of living striated muscle during contraction. *J. Mol. Biol.* 25:31–45.
32. Daniel, T. L., A. C. Trimble, and P. B. Chase. 1998. Compliant realignment of binding sites in muscle: transient behavior and mechanical tuning. *Biophys. J.* 74:1611–1621.

33. Campbell, K. S. 2006. Filament compliance effects can explain tension overshoots during force development. *Biophys. J.* 91:4102–4109.

34. Campbell, K. S. 2006. Tension recovery in permeabilized rat soleus muscle fibers after rapid shortening and restretch. *Biophys. J.* 90:1288–1294.

35. Ford, L. E., A. F. Huxley, and R. M. Simmons. 1977. Tension responses to sudden length change in stimulated frog muscle fibres near slack length. *J. Physiol.* 269:441–515.

36. Cecchi, G., P. J. Griffiths, and S. Taylor. 1982. Muscular contraction: kinetics of crossbridge attachment studied by high-frequency stiffness measurements. *Science.* 217:70–72.

37. Cecchi, G., P. J. Griffiths, and S. Taylor. 1986. Stiffness and force in activated frog skeletal muscle fibers. *Biophys. J.* 49:437–451.

38. Brunello, E., M. Caremani, …, M. Reconditi. 2014. The contributions of filaments and cross-bridges to sarcomere compliance in skeletal muscle. *J. Physiol.* 592:3881–3899.

39. Wang, L., and M. Kawai. 2013. A re-interpretation of the rate of tension redevelopment (k(TR)) in active muscle. *J. Muscle Res. Cell Motil.* 34:407–415.

40. Colombini, B., M. Nocella, …, G. Cecchi. 2010. Is the cross-bridge stiffness proportional to tension during muscle fiber activation? *Biophys. J.* 98:2582–2590.

41. Linari, M., G. Piazzesi, and V. Lombardi. 2009. The effect of myofilament compliance on kinetics of force generation by myosin motors in muscle. *Biophys. J.* 96:583–592.

42. Linari, M., E. Brunello, …, M. Irving. 2015. Force generation by skeletal muscle is controlled by mechanosensing in myosin filaments. *Nature.* 528:276–279.

43. Wigston, D. J., and A. W. English. 1992. Fiber-type proportions in mammalian soleus muscle during postnatal development. *J. Neurobiol.* 23:61–70.

44. Eng, C. M., L. H. Smallwood, …, R. L. Lieber. 2008. Scaling of muscle architecture and fiber types in the rat hindlimb. *J. Exp. Biol.* 211:2336–2345.

45. Li, F., D. Buck, …, H. L. Granzier. 2015. Nebulin deficiency in adult muscle causes sarcomere defects and muscle-type-dependent changes in trophicity: novel insights in nemaline myopathy. *Hum. Mol. Genet.* 24:5219–5233.

46. Hu, Z., D. W. Taylor, …, K. A. Taylor. 2016. Structure of myosin filaments from relaxed *Lethocerus* flight muscle by cryo-EM at 6 Å resolution. *Sci. Adv.* 2:e1600058.

47. Tonino, P., B. Kiss, …, H. Granzier. 2017. The giant protein titin regulates the length of the striated muscle thick filament. *Nat. Commun.* 8:1041.

48. Granzier, H. L., and S. Labeit. 2005. Titin and its associated proteins: the third myofilament system of the sarcomere. *Adv. Protein Chem.* 71:89–119.

49. Kampourakis, T., Z. Yan, …, M. Irving. 2014. Myosin binding protein-C activates thin filaments and inhibits thick filaments in heart muscle cells. *Proc. Natl. Acad. Sci. USA.* 111:18763–18768.

50. McKillop, D. F., and M. A. Geeves. 1993. Regulation of the interaction between actin and myosin subfragment 1: evidence for three states of the thin filament. *Biophys. J.* 65:693–701.

51. Lehman, W., P. Vibert, …, R. Craig. 1995. Steric-blocking by tropomyosin visualized in relaxed vertebrate muscle thin filaments. *J. Mol. Biol.* 251:191–196.

52. Irving, M. 2017. Regulation of contraction by the thick filaments in skeletal muscle. *Biophys. J.* 113:2579–2594.

53. Huxley, H. E., and W. Brown. 1967. The low-angle x-ray diagram of vertebrate striated muscle and its behaviour during contraction and rigor. *J. Mol. Biol.* 30:383–434.

54. Reconditi, M., M. Linari, …, V. Lombardi. 2004. The myosin motor in muscle generates a smaller and slower working stroke at higher load. *Nature.* 428:578–581.